RSC Advances

ROYAL SOCIETY OF CHEMISTRY

www.rsc.org/advances

Porous wide band gap $BiNbO_4$ ceramic nanopowder synthesised by low temperature solution-based method for gas sensing applications

C. Balamurugan, D.-W. Lee,*

MEMS and Nanotechnology Laboratory, School of Mechanical Systems Engineering, Chonnam National University, Gwangju 500757, Republic of Korea.

AR. Maheswari

PG and Research Department of Chemistry, J.J. College of Arts and Science, Pudukkottai- 622 422, India.

M. Parmar

Department of Instrumentation & Applied Physics, Indian Institute of Science, Bangalore 560012, India.

Graphical Abstract

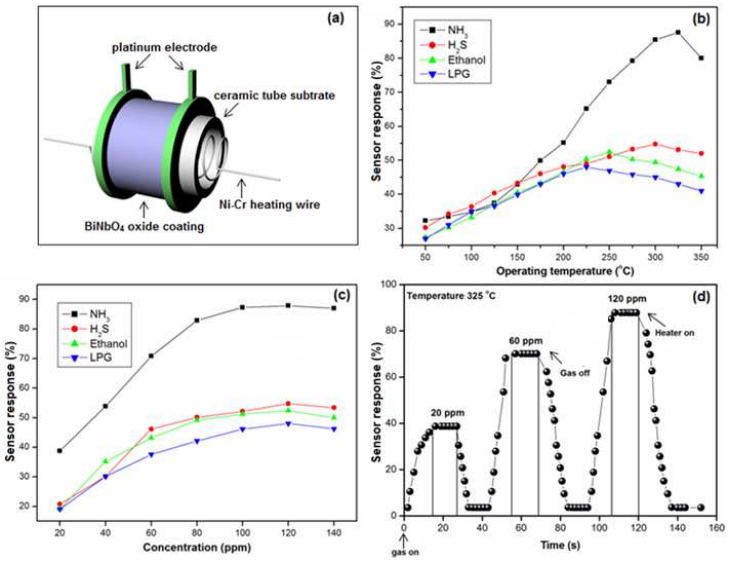

Abstract

In this study, we report the gas sensing behavior of $BiNbO_4$ nanopowder prepared by low temperature simple solution-based method. Before sensing behaviour study, the as-synthesized nanopowder was characterized by X-ray diffraction, scanning electron microscopy, transmission electron microscopy, UV–diffuse reflectance spectroscopy, impedance analysis, and surface area measurement. The NH_3 sensing behavior of $BiNbO_4$ was then studied by temperature modulation (50–350 °C) as well as concentration modulation (20–140 ppm). At the optimum operating temperature of 325 °C, the sensitivity was measured to be 90%. The cross-sensitivity of as-synthesized $BiNbO_4$ sensor was also investigated by performing sensing behavior of other gases such as hydrogen sulphide (H_2S), ethanol (C_2H_5OH), and liquid petroleum gas (LPG). Finally, selectivity of the sensing material toward NH_3 was characterized by observing the sensor response with gas concentrations in the range 20–140 ppm. The response and recovery time for NH_3 sensing at120 ppm were about16 s and about17 s, respectively.

Keywords: $BiNbO_4$; gas sensor; wide band gap ceramic; p-type semiconductor.

* Corresponding author. Email: mems@jun.ac.kr

Introduction

ABO_4 compounds (A = Bi^{3+} or Sb^{3+} and B = Nb^{5+}, Ta^{5+} or Sb^{5+}) have received much attention owing to their unique properties such as ferroelectrics and anti-ferroelectrics with the stibiotantalite structure, consisting of a layer of vertex sharing and distorted BO_6 octahedral parallel to the (001) plane of the orthorhombic unit cell. Moreover, they possess excellent piezoelectric, pyroelectric, and electro-optic properties at room temperature [1]. Among the various ABO_4 compounds, bismuth-based microwave dielectric ceramic has stimulated significant research interest owing to its unique structural characteristics, electrical properties and promising applications in the field of multilayer capacitors [2–4]. From the viewpoint of gas sensor applications, $BiNbO_4$ could be considered as a promising candidate for future developments of sensing materials. According to the sensing mechanisms of conductance-based gas sensors, the overall sensing performance is determined by the charge transfer between the adsorbed species and the sensing material [5]. With the progress of gas sensing research, porous structure with a high specific surface area and an easy surface accessibility has been found to significantly improve the gas sensing properties. Until now, $BiNbO_4$ materials are generally synthesized by solid-state processes, which are quite strenuous and require high reaction temperature. The high operating temperature in material preparation leads to large agglomerations of particles and low surface area which results in to their poor gas sensing behavior.

Ammonia (NH_3) is one of the most used gases in many chemical industries, agricultural industries including fertilizer factories, food industries petroleum industries, rubber industries, lather industries as well as industrial refrigeration systems [6]. Ammonia also contributes

significantly to the nutritional needs of terrestrial organisms by serving as a precursor of food and fertilizers. It is also a building block for the synthesis of many pharmaceuticals. Despite its usefulness, NH_3 is both caustic and hazardous to humans, especially when its concentration exceeds threshold value (TLV) of 25 ppm [7]. Its exposure may develop a burning sensation in eyes, nose, and throat. The Permissible exposure limits (PELs) set by Occupational safety and health administration (OSHA), USA – is around 50 ppm. To prevent the serious accidents caused by the NH_3 gas leakage, the compact NH_3-sensing devices that can be placed on various emitting sites are required. Although, there are ample reports published on NH_3 sensing, novel materials are explored every day in order to obtain better sensing performance.

In the present paper, we are reporting NH_3 sensing behavior of novel material-$BiNbO_4$ nanopowder. To the best of our knowledge, the detailed gas sensing behaviour of porous $BiNbO_4$ nanostructures prepared by a chemical-based method is not reported yet. The sensing response of $BiNbO_4$-based material was studied by variation in its electrical resistance in the air and reducing gas environments. The change in resistance is caused by the transfer of charges as a result of adsorption between gas molecules and the metal oxide semiconductor surface. The $BiNbO_4$ nanopowder-based sensor realizes the selective detection of NH_3 to other interference gases such as H_2S, ethanol and LPG.

- Preparation of $BiNbO_4$ nanopowder

A simple yet reliable and safer chemical-based procedure was employed for the synthesis of $BiNbO_4$ nanopowder using common reagents like bismuth nitrate, niobium ammonium oxalate, tartaric acid. All the reagents used in the experiments are analytically pure which ensures high

purity $BiNbO_4$ nanopowder. Hydrated niobium was formed by the dissolution of the niobium ammonium oxalate in water and precipitated as niobium hydroxide by adding ammonium hydroxide. The resulting precipitate was washed using distilled water and dried; the prepared niobium hydroxide was then assyaed at 1,200 °C for 2 h to estimate the amount of niobium oxide present in the niobium hydroxide. The required amount of niobium hydroxide was dissolved in an aqueous tartaric acid [TA, $HO_2CCH(OH)CH(OH)CO_2H$] solution in TA to Nb ratio of 2:1. Then, a stoichiometric ratio of bismuth nitrate was added to this precursor mixture with a Bi to Nb ratio of 1:1, followed by drop wise addition of 0.2 M PVA solution and 0.1 M ethylene glycol solutions with constant stirring, and the pH value of the final solution was adjusted to 7 using NH_4OH solution. The resulting solution was heated on a hot plate, and after the complete gelation, hot plate temperature was increased to 250 °C to obtain dried black fluffy mass. The porous $BiNbO_4$ nanopowder was successfully obtained by the calcination of the $BiNbO_4$ precursor at 500 °C in a muffle furnace for 2 h. Thermal behavior of the dried precursor was studied in the air atmosphere by TG/DTA using a Pyris Diamond thermal gravimetric analyzer. The calcined sample is characterized by X-ray powder diffraction using CuKα sources (XRD, X'Pert pro), scanning electron microscopy (FE-SEM, JSM-7500F), transmission electron microscopy (TEM, JEOL JEM-2100F), Brunauer-Emmett-Teller surface area measurement (BET, Micrometritics, ASAP 2020), UV-vis diffuse reflectance spectroscopy (DRS, Varian-Cary 5000) and impedance analysis (Model-micro auto lab type III), respectively.

- Results and discussion

Figure 1a shows the simultaneous TGA and DTA plots for the dried precursor. As per TGA data, the total weight loss is around 35% over a temperature range of room temperature to 900 °C.

The endothermic (negative) peak on the DTA curves centered at 128 °C, with drastic weight loss in the TG curve, corresponds to the evaporation of residual water and chemically bound water in the precursor sample. As the process of heating is continued, two distinguishable exothermic transformations observed at 344 and 421 °C. This might be due to the reaction of nitrates with tartaric acid and decomposition of remaining organic constituents in the precursor. In order to obtain the orthorhombic phase of the powder, the calcination condition was optimized to be 500 °C for 3 h. Figure 1b shows the XRD pattern of calcinated $BiNbO_4$ powder. It can be seen that all the peaks in the XRD spectrum perfectly indexed according to the orthorhombic phase of $BiNbO_4$ with lattice constants a, b, and c of 4.979, 11.68, and 5.674Å (JCPDS 16-0295). The optimized calcination temperature to obtain pure orthorhombic $BiNbO_4$ was considerably lower compared to all the previous reports [1, 3, 8, and 9]. From the Scherrer equation, the average crystallite size of $BiNbO_4$ was calculated to be 23 nm.

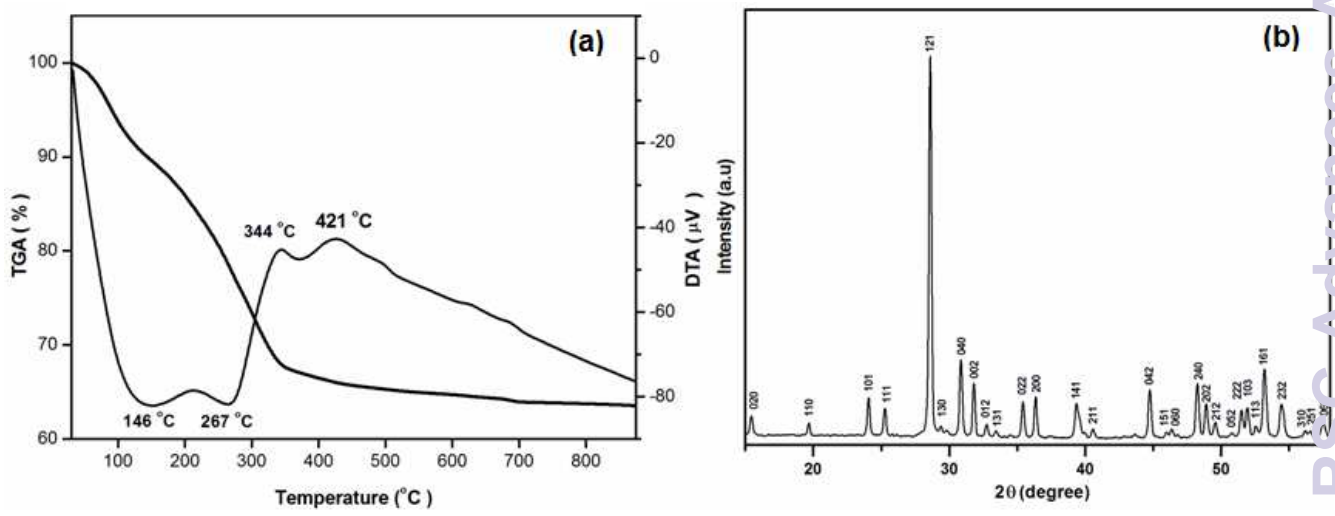

Figure 1. Simultaneous TG/DTA plots obtained for the $BiNbO_4$ precursor sample (a) and XRD pattern of $BiNbO_4$ precursor powder calcined at 500 °C for 3h.

The FE-SEM image clearly shows the porous morphology of the as-synthesized product (Fig. 2a). The porous morphology facilitates analyte gas to diffuse easily toward the entire surface of the material and improves surface interactions. This, in turn, improves the rate of reaction of gas molecules with the adsorbed oxygen on the surface. The TEM image of $BiNbO_4$ nanopowder (Fig. 2b) indicates the formation of well-dispersed spherical shape particles with an average diameter of ~30 nm. The specific surface area (41.27 m^2/g) of calcinated $BiNbO_4$ nanopowder was estimated by the BET method.

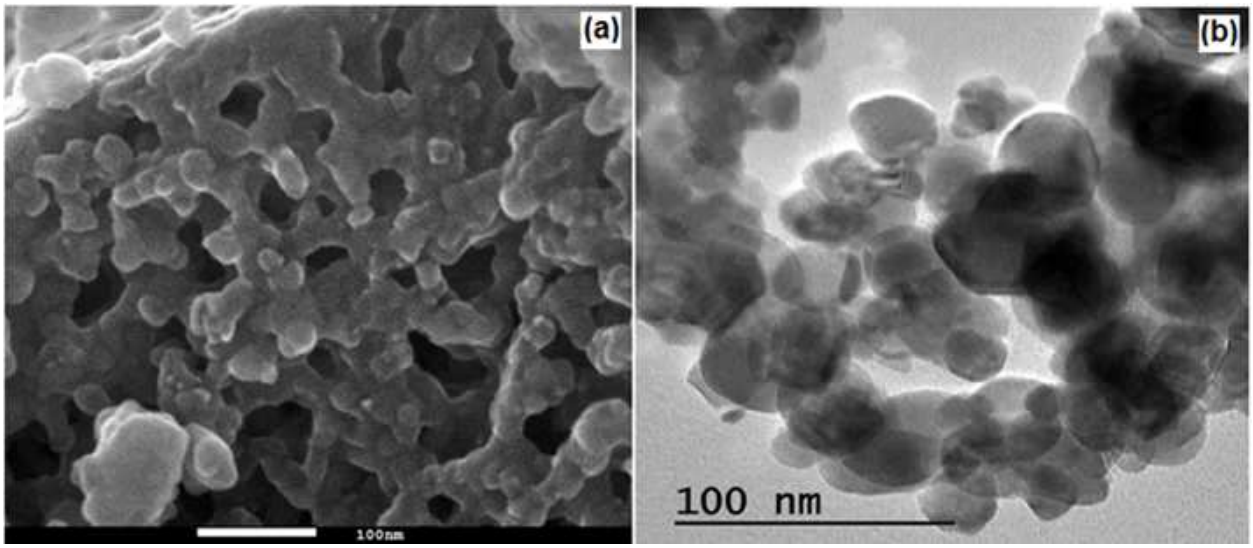

Figure 2. FE-SEM images of $BiNbO_4$ (a) and HR-TEM micrograph of $BiNbO_4$ (b).

The porosity of the synthesized $BiNbO_4$ nanopowder was also studied by mixing nanopowder with a few drops of polyvinyl alcohol solution. The mixture was pressed into a pellet and then heat-treated at 400 °C to remove the residual polymer. The porosity was calculated by using the following relation [10]:

$$P = 1-(d/dx) \qquad (1)$$

Where *d* is m/V calculated from the dimensions and mass of the pellet. X-ray density (*dx*) was calculated using the following equation:

$$dx = 8M/Na^3 \qquad (2)$$

where M, N, and a are the molecular weight, Avogadro's number (6.023×10^{23} atoms/mole), and lattice constant, respectively. The porosity of the sample was 57%, leading to the adsorption of gas molecules in the pores yielding a highly sensitive material.

The UV–vis absorption spectrum of the products is shown in Fig. 3a. The band gap of the sample can be calculated by the following equation: $(\alpha h\nu)^2 = B\times(h\nu - E_g)$ where α is the absorption coefficient, $h\nu$ is the photon energy, B is a constant, and E_g is the band gap. The $(\alpha h\nu)^2$ vs. $h\nu$ curve is also shown in Fig. 3b. Extrapolation of the linear portion of the energy axis at $(\alpha h\nu)^2 = 0$ gave the E_g value of 3.2 eV. The electrical conductivity of $BiNbO_4$ was evaluated from complex impedance spectra (Fig. 3c) and expressed as a function of temperature from 30 to 175 °C in dry air. The resistance *R* of the sample was obtained from the intercept on the *x*-axis of the complex impedance plot. The Arrhenius plot (Fig. 3d) shows that the observed temperature dependence on electrical conductivity is similar to those observed in semiconductor oxide systems. The activation energy of the conduction process was calculated from the slope of log σ vs. 1/T plot. In the temperature range of 30-175 °C, the activation energy of $BiNbO_4$ was 0.29 eV.

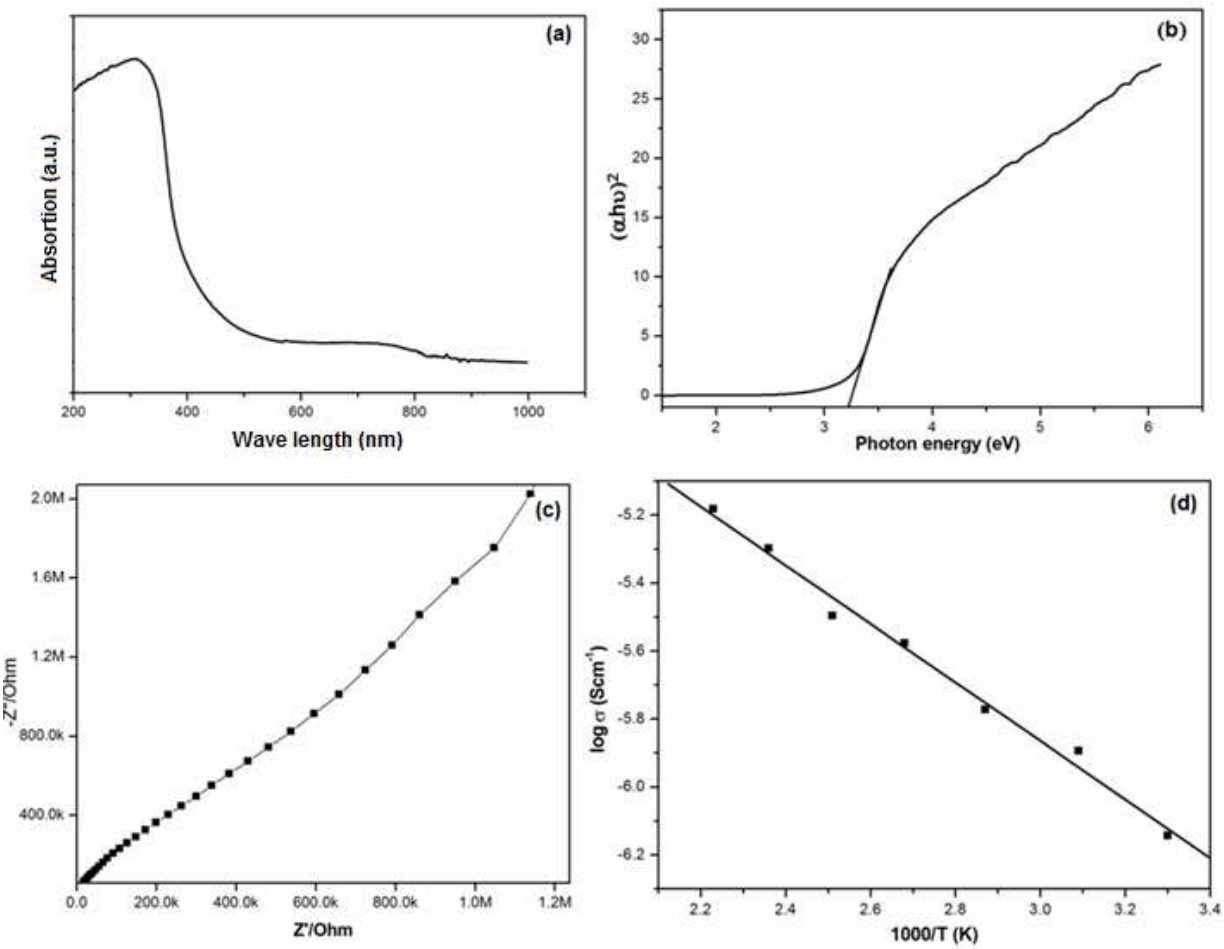

Figure 3. Experimental results of UV–vis DRS (a), $(\alpha h\nu)^2$ vs. hν cures (b), impedance spectrum (c), and the Arrhenius plot of $BiNbO_4$nanopowder (d).

For gas sensing measurement, the prepared $BiNbO_4$ nanopowder was mixed with α-terpineol to form a paste and then coated on an Al_2O_3 ceramic tube with a pair of platinum electrode on each end. In order to provide required operating temperature while gas sensing, a small nichrome (NiCr) alloy coil was placed inside the tube to function as a heater. The schematic of a sensor element used for the gas response studies is shown in Fig. 4(a). A detailed

description of the sensor device, electrical circuit, and preparation method can be followed from our previous report [11]. The brief sensing analysis with the sensing element is as follows. In the first step, the resistivity of the sample was measured in the air (R_a), i.e., prior to admitting test gas inside the sealed chamber as well as in the presence of a test gas (R_g). It was observed that the $BiNbO_4$ nanopowder-based sensor offered an increased resistance in the presence of reducing gases. This behavior exhibits p-type semiconductor nature for the $BiNbO_4$ nanopowder. The sensitivity of the sensors S was calculated using the following mathematical expression: $S = R_a/R_g$ [12]. Figure 4(b) shows the dynamic gas sensing characteristics of $BiNbO_4$ nanopowder towards NH_3, H_2S, ethanol, and LPG as a function of operating temperatures. Among these gases, NH_3 is the main test gas whereas the other the response of other gas is analyzed in order to observe the cross-sensitivity effect. Here, the response was defined as the change in resistance before and after the admittance of reducing gas. In order to obtain the optimum operating temperature (T_{opt}) for NH_3, the sensor response was analyzed over a temperature range of 50–350 °C keeping the gas concentration constant. This analysis was term as temperature modulation study. The T_{opt} for NH_3 sensing was found at the temperature of about 325 °C. The T_{opt} for H_2S (54%), ethanol (46%) and LPG (40%) sensing was around 300, 250, and 225 °C, respectively. The behavior of sensor in varying gas concentration is also an important analysis. It gives the linear working range, in terms of concentration, of a sensor. This study can be termed as concentration modulation. The gas sensing response of $BiNbO_4$ as a function of concentrations (20–140 ppm) of test gases at their T_{opt}(NH_3-325 °C, H_2S-305 °C, ethanol-250 °C, and LPG-225 °C) is shown in Fig. 4(c). The sensor response was remarkably high when exposed to NH_3 at its T_{opt} (i.e., 325 °C) compared to the sensor response of other gases at their respective

T_{opt}s. The lower sensor response of other test gases (such as H_2S, ethanol, and LPG) even at their own T_{opt}s clearly indicates a selective response of the sensor towards ammonia. This selective response was owing to the complete oxidization of NH_3 on the sensor surface, thereby changing the conductivity of the sensor element drastically compared to other gases.

Figure 4(d) shows the response variations in the $BiNbO_4$ sensor upon exposure to NH_3 gas injection and refreshing. The measurements were performed by injecting varying amounts of NH_3 gas into the sealed chamber, followed by refreshing (i.e., stopping gas injection and flushing of residual gases) at 325 °C. The measured response for 20, 60, and 120 ppm NH_3 gas was ~38%, 70%, and 87%, respectively. The NH_3 gas attained maximum response within 16 s, and its recovery time was less than 17 s. The fast response as well as recovery of the above discussed sensor can be attributed to the large surface area of the material and rapid adsorption/desorption rate due to smaller molecular weight of NH_3 compared to other gases such as hydrocarbon gases. The relatively fast response is consistent with the hypothesis of a surface effect, especially related to the ammonia adsorption on the $BiNbO_4$ surface and can be correlated to the surface morphology. High porosity increases the number of accessible sites for the adsorption of molecules, resulting in a high response to NH_3. The electric dipole moment of ammonia is 5.0×10^{-30} C·m, and this high polarity would easily attract the metal oxide-based positively charged nanoparticles. In addition, response properties and selectivity depend on the nature of active sites in structure of the sensor surface. Moreover, surface acidity of metal oxides may play an important role in selective sensing of NH_3. Taking into account the fact that NH_3 is a basic molecule, the result can be explained as follows. The surface of the oxides with more electronegative metal (i.e., more acidic (Nb)) strongly interacts with basic NH_3 molecules,

resulting in high response to NH_3. The high sensitivity and the low detection level of the sensor are very interesting points for its practical applications. Moreover, it can detect a large range of ammonia concentrations. The proposed $BiNbO_4$–based gas sensor exhibited improved selectivity compared to the other metal oxide type NH_3 gas sensors. The improved selectivity obtained with the $BiNbO_4$ sensor makes it a valuable tool in the determination of NH_3 gas concentrations. Considering the wide use of ammonia, this sensor can be utilized in the analysis of food and beverage products, industrial refrigerant, and in the selective determination of NH_3 levels in the various sites such as nitrogenous fertilizers as well as other industries having typically higher concentration of other interfering gases (H_2S, ethanol, and LPG). A comparison between the NH_3 sensing performances of the $BiNbO_4$ sensor and literature reports is summarized in Table.1. $BiNbO_4$ sensor for detection of ammonia gas shows the better detection limits than previously reported devices.

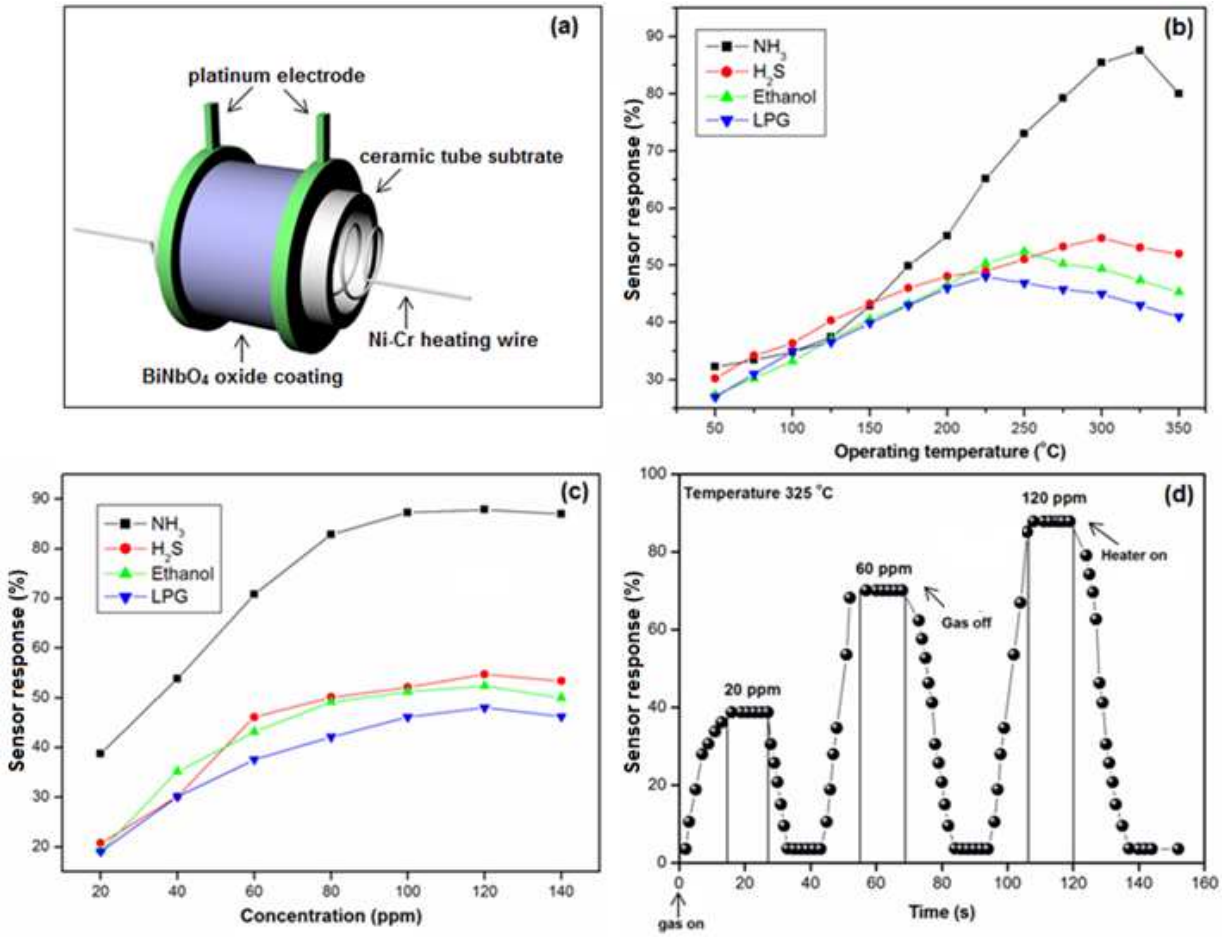

Figure 4. (a) Schematic of sensor element used for the gas response studies, (b) dynamic gas sensing characteristics of $BiNbO_4$ nanopowder towards NH_3, H_2S, ethanol, and LPG as a function of operating temperatures, (c) gas sensing response of $BiNbO_4$ as a function of concentrations (20–140 ppm) and (d) response and recovery time of the sensor to different concentrations of NH_3.

Tabel.1

Material	NH_3 concentration (ppm)	Sensor response	Response & recovery time	Reference
Pd-$LaCo_{0.8}Fe_{0.2}O_3$	200	97 (300 ^oC)	8-20s	[13]
Zr and $CoWO_4$	1,000	50 (700 ^oC)	1-3s	[14]
Pt-WO_3	4,000	45 (350 ^oC)	1m-5mintes	[15]
$Co_{0.8}Ni_{0.2}Fe_2O$	250	68 (250 ^oC)	20-70s	[16]
$CuNb_2O_6$	500	56 (300 ^oC)	15-25s	[17]
WO_3nano particle	500ppb	66 (300 °C)	18-15mintes	[18]
Carbon nanotube coated with Co	14 to 900	75(900ppm at room temperature)	30 to50/200 to500s	[19]
$BiNbO_4$	120	87 (325 ^oC)	16-17s	Thiswork

Acknowledgements

This study was supported by a grant of the KHT R&D Project (HI13C1527) and the NRF grant (No. 2012R1A2A2A01014711) funded by the Korea government.

References

[1] Liou .Y.C, Tsai .W.C and Chen .H.M, Low-temperature synthesis of $BiNbO_4$ ceramics using reaction-sintering process *Ceramic International*, 2009, 35, 2119-2122.

[2] Liu .D, Liu .Y, Huang .S.Q and Yao .X, Phase structure and dielectric properties of Bi_2O_3-ZnO-Nb_2O_5-based dielectric ceramics *Journal of American Chemical Society* 1993,76, 2129-2132.

[3] Ling .H.C, Yan .M.F and Rhodes .W.W, 1990 High dielectric constant and small temperature coefficient bismuth-based dielectric compositions *Journal of materials Research*, 1990, 5, 1752-1762.

[4] Kim .E.S and Choi. W, Effect of phase transition on the microwave dielectric properties of $BiNbO_4$, *Journal of European Ceramic Society*, 2006, 26, 1761-1766.

[5] Timmer .B and Olthuis .W, Berg, Ammonia sensors and their applications-a review, *Sensors and Actuators B: Chemical*, 2005, 107, 666-677.

[6] Nagai .T, Tamura .S and Imanaka .N, Solid electrolyte type ammonia gas sensor based on trivalent aluminum ion conducting solids *Sensors and Actuators B: Chemical*, 2010, 147, 735-740.

[7] Wetchakuna .K, Samerjaia .T, Tamaekonga .N, Liewhirana .C, Siriwonga .C, Kruefua .V, Wisitsoraatb .A, Tuantranontb .A, Phanichphant .S, Semiconducting metal oxides as sensors for environmentally hazardous gases, *Sensors and Actuators B: Chemical*, 2011, 160, 580-591.

[8] Wang .N, Zhao .M.Y, Yin .Z.W and Li .W, Low-temperature synthesis of h-$BiNbO_4$ powder by citrate sol–gel method, *Maerals Letters*, 2003, 57, 4009-4013.

[9] Radha .R, Gupta .U.N, Samuel .V, Muthurajan .H, Kumar .H.H, Ravi .V A co-precipitation technique to prepare $BiNbO_4$ powders, *Ceramic International*, 2008, 34, 1565-1567.

[10] Rezlescu .N, Rezlescu .E and Tudorache .F Popa .P.D, Gas sensing properties of porous Cu,-Cd and Zn ferrities, *Romanian Repots in Physics*, 2009, 61, 223-234.

[11] Balamurugan .C and Lee .D.W, A selective NH_3 gas sensor based on mesoporous p-type NiV_2O_6semiconducting nanorods synthesized using solution method, *Sensors and Actuators B: Chemical*, 2014, 192, 414-422.

[12] Anjali Chatterjee, Partha Bhattacharjee, Roy .N.K, Kumbhakar .P, Usage of nanotechnology based gas sensor for health assessment and maintenance of transformers by DGA method, *International Journal Of Electrical Power and Energy Systems,* 2013, 45, 137–141.

[13] Chaudhari .G, Jagtap .S, Gedam .N, Pawar .M and Sangawar .V, Sol–gel synthesized semiconducting $LaCo_{0.8}Fe_{0.2}O_3$-based powder for thick film NH_3 gas sensor *Talanta*, 2009, 78, 1136-1140.

[14] Diao .Q, Yang .F, Yin .C, Li .J, Yang .S, Liang .X and Geyu Lu, Ammonia sensors based on stabilized zirconia and $CoWO_4$ sensing electrode, *Solid State Ionics*, 2012, 225, 328-331.

[15] Srivastava .V and Jain .K, Highly sensitive NH_3 sensor using Pt catalyzed silica coating over WO_3 thick films, *Sensors and Actuators B: Chemical*, 2008, 133, 46-52.

[16] Gedam .N, Padole .P, Rithe .S and Chaudhari .G Ammonia gas sensor based on a spinel semiconductor, $Co_{0.8}Ni_{0.2}Fe2O_4$, *Journal of Sol Gel Science and Technology*, 2009, 50, 296-300.

[17] Biswas .S and Pramanki .K, Study on gas sensing behaviour of nano sized $CuNb_2O_6$ toward ammonia, hydrogen and liquid petroleum gas, *Sensor and Actuators B: chemical*, 2008, 133, 449-455.

[18] Dzung Viet DAO, Kyoji Shibuya, Tung Thanh Bui, Susumu Sugiyama,Micromachined NH_3 Gas Sensor with ppb-level Sensitivity Based on WO_3 Nanoparticles Thinfilm, *Procedia Engineering,* 2011, 25, 1149-1152.

[19] Lich Quang Nguyen, Pho Quoc Phan, Huyen Ngoc Duong , Chien Duc Nguyen and Lam Huu Nguyen, Enhancement of NH_3 Gas Sensitivity at Room Temperature by Carbon Nanotube-Based Sensor Coated with Co Nanoparticles, *Sensors*, 2013, *13*, 1754-1762.

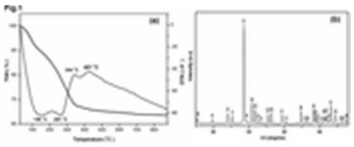

7x2mm (600 x 600 DPI)

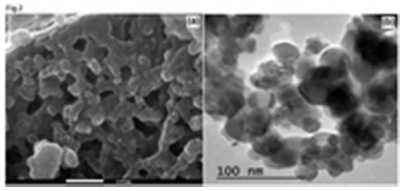

8x3mm (600 x 600 DPI)

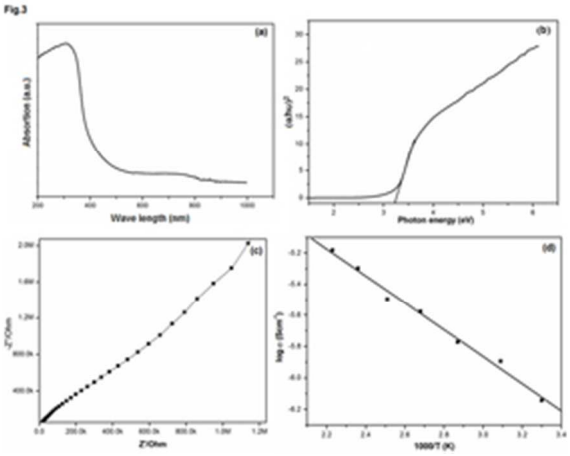

12x9mm (600 x 600 DPI)

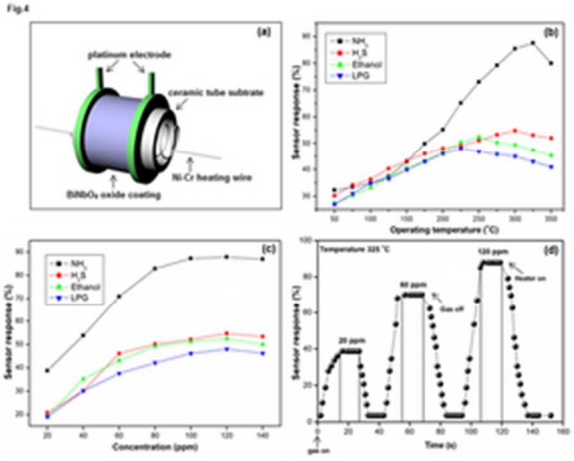

12x9mm (600 x 600 DPI)